Carbohydrate Polymers 117 (2015) 950–956

Contents lists available at ScienceDirect

Carbohydrate Polymers

journal homepage: www.elsevier.com/locate/carbpol

Revealing the structures of cellulose nanofiber bundles obtained by mechanical nanofibrillation via TEM observation

Wenshuai Chen, Qing Li, Jun Cao, Yixing Liu, Jian Li, Jiangshuai Zhang, Shuiyang Luo, Haipeng Yu*

Key Laboratory of Bio-based Material Science and Technology, Ministry of Education, Northeast Forestry University, No.26 Hexing Rd., Harbin 150040, PR China

ARTICLE INFO

Article history:
Received 9 June 2014
Received in revised form 3 October 2014
Accepted 6 October 2014
Available online 23 October 2014

Keywords:
Cellulose nanofibers
Bundles
Transmission electron microscopy
Structures

ABSTRACT

To reveal the structures of cellulose naonfiber bundles extracted from lignocellulosic pulps and prepared by mechanical nanofibrillation methods, the samples were systematically investigated by transmission electron microscopy (TEM) observation. First, high magnification and high resolution TEM images were obtained starting from one end of the bundles. The imaging position was then carefully shifted along the length of the bundles until the other end was reached. Finally, a series of TEM images were integrated through image processing and analyzed. The cellulose nanofiber bundles displayed ribbon-like structures, which were organized with parallel aligned cellulose nanofibers 2–5 nm in width. The length of the bundles was >11 μm. The bundles were interconnected with other nanofibers and nanofiber bundles, forming entangled, web-like networks in suspension. Evidence demonstrating the existence of twisted bundle morphologies was also presented.

1. Introduction

In the last decade, nanocellulose has been the subject of intense research (Eichhorn, 2011; Habibi, Lucia, & Rojas, 2010; Isogai, 2013; Isogai, Saito, & Fukuzumi, 2011; Klemm et al., 2011; Moon, Martini, Nairn, Simonsen, & Youngblood, 2011; Siró & Plackett, 2010) because its unique physiochemical properties are different from those of cellulose pulps. Various applications of nanocellulose are anticipated in transparent films (Nogi, Iwamoto, Nakagaito, & Yano, 2009; Nogi & Yano, 2008; Yano et al., 2005), reinforcing fillers for polymers (Capadona, Shanmuganathan, Tyler, Rowan, & Weder, 2008; Capadona et al., 2007), aerogels (Chen et al., 2014; Chen, Yu, Li, Liu, & Li, 2011; Pääkkö et al., 2008), templates (Kelly, Giese, Shopsowitz, Hamad, & MacLachlan, 2014; Olsson et al., 2010; Shopsowitz, Qi, Hamad, & MacLachlan, 2010), separation membranes (Metreveli et al., 2014), and many others. Long and flexible cellulose nanofibers can be produced by the nanofibrillation of chemically purified cellulose pulps using a grinder (Abe, Iwamoto, & Yano, 2007; Abe & Yano, 2009; Abe & Yano, 2010), a high-pressure homogenizer (Herrick, Casebier, Hamilton, & Sandberg, 1983; Turbak, Snyder, & Sandberg, 1983), a blender (Uetani & Yano, 2010; Uetani & Yano, 2013), or a high intensity ultrasonicator (Chen et al., 2011b; Chen et al., 2011c; Zhao, Feng, & Gao, 2007). Compared with mechanical nanofibrillation, chemical or enzyme pretreatment followed by nanofibrillation technique, was reported to reduce the production cost, by decreasing the number of treatments through the nanofibrillation facilities (Abe et al., 2007; Chen et al., 2011b, 2011c; Pääkkö et al., 2007). It is well known that cellulose nanofibers with 2–5 nm widths can be exacted after mechanical nanofibrillation (Eichhorn, 2011; Habibi et al., 2010; Isogai, 2013; Isogai et al., 2011; Klemm et al., 2011; Moon et al., 2011; Siró & Plackett, 2010). However, cellulose nanofibers usually self-organized into bundles or aggregates during the drying process. (Eichhorn, 2011; Habibi et al., 2010; Isogai, 2013; Isogai et al., 2011; Klemm et al., 2011; Moon et al., 2011; Siró & Plackett, 2010) because of the complicated physical and chemical interactions between the nanofibers. Thus, the structures of cellulose nanofiber bundles play a critical role in the understanding and application of cellulose nanofibers.

Scanning electron microscopy (SEM) has exclusively been utilized for the structural analysis of cellulose nanofibers and nanofiber bundles. Coating the surfaces of samples with gold or platinum before SEM observation is needed to avoid charging. However, the coating most likely broadens the nano-sized structures. In addition, the cellulose nanofibers inside the bundles probably self-aggregate into thick nanofibers with widths of 12–50 nm or more when they are dried into a thin sheet for SEM observation (Abe et al., 2007; Abe & Yano, 2009; Abe & Yano, 2010; Chen et al.,

* Corresponding author.
E-mail address: yuhaipeng20000@gmail.com (H. Yu).

http://dx.doi.org/10.1016/j.carbpol.2014.10.024
0144-8617/

2011b, 2011c). Thus, SEM can not clearly reveal the real structures of cellulose nanofiber bundles. Compared with conventional SEM, the resolution of atomic force microscopy (AFM) and transmission electron microscopy (TEM) is high, and it is not necessary to coat the sample surfaces before observation. Conventional TEM and AFM analyses typically reveal the widths of single cellulose nanofibers, slender bundles, and web-like entangled structures. Few works, however, have utilized TEM or AFM to characterize the length of the bundles. Because the bundles are thin and long, their entire length can not be included when they are observed at high magnification. Decreasing the magnification, however, prohibits the clear display of the bundle structures because of the low resolution. For these reasons, the structures along the whole length of the bundles have never been systematically investigated.

The plant cell walls consist of a rigid, multi-layered and higher order structure in which cellulose microfibril bundles mutually adhere by means of strong cohesive forces derived from their hydroxyl groups. The microfibrils within the cell walls of cellulosic materials exhibit twisted morphologies (Hanley, Revol, Godbout, & Gray, 1997; Khandelwal & Windle, 2014). When the cell walls are disintegrated and release the cellulose nanofibers and nanofiber bundles, whether the twisted bundle structures become flat due to mechanical nanofibrillation or still unchanged, remains unclear. Therefore, high resolution characterization along the full lengths of the bundles is important to show their real structures.

Here, the structures of cellulose nanofiber bundles were revealed by a careful integration of high resolution TEM images recorded along the length of the bundles. The ribbon-like bundles were long and flexible. Impressively, the bundles were organized with parallel aligned cellulose nanofibers. Evidence demonstrating the presence of twisting in the bundles was also presented.

2. Experimental

2.1. Materials

Wood, bamboo, rice straw, corn straw and newspaper were used as sources of native cellulose fibers. Wood powders from poplar wood were sieved with 60 mesh. Mature culms of Moso bamboo were collected from Zhejiang Province, China. The rice straw and corn straw were collected from local farms in Heilongjiang Province, China; only stems cut into approximately 10 mm lengths were used. Commonly-used newspapers were collected. The newspaper was torn into small pieces before use. All samples were air-dried and stored at room temperature. Benzene, ethanol, sodium chlorite, acetic acid, potassium hydroxide, and other chemicals were of laboratory grade and used without further purification.

2.2. Removal of matrixes

Chemical purification of raw materials was performed according to the literature with minor modifications (Chen et al., 2011b,c). Briefly, 2 g samples were dewaxed in a Soxhlet apparatus with a 2:1 (v/v) mixture of benzene/ethanol for 6 h. Afterward, lignin in the samples was removed using an acidified sodium chlorite solution at 75 °C for 1 h; this process was repeated three times. Next, the samples were treated with 3 wt% potassium hydroxide at 90 °C for 1 h to remove large amounts of hemicelluloses. To produce highly purified cellulose, the samples were further treated with an acidified sodium chlorite solution at 75 °C for 1 h followed by treated with 8 wt% potassium hydroxide at 90 °C for 1 h. This resulted in purified cellulose pulps, and the hemicellulose content, which was measured based on previous method (Chen et al., 2011c), was in the range of 13–18%, depending on the raw materials. Lignin was totally removed during the chemically purified process.

2.3. Fibrillation of cellulose pulps using a blender

The chemically purified cellulose suspension (250 mL) with fiber contents of 0.2 wt% was fibrillated using a common domestic blender. The agitation time was 20 min.

2.4. Fibrillation of cellulose pulps using an ultrasonicator

The chemically purified cellulose suspension (100 mL) with fiber contents of 0.2 wt% was fibrillated using a high intensity ultrasonicator (JY99-IIDN, Ningbo Scientz Biotechnology Co., China) at 1200 W for 20 min. This procedure was based on the previous work (Chen et al., 2011b, 2011c).

2.5. Fibrillation of cellulose pulps using a high-pressure homogenizer

To avoid blocking of the high-pressure homogenizer by the big cellulose fibers, the chemically purified cellulose suspension with fiber contents of 0.2 wt% was subjected to pre-fibrillation using a high intensity ultrasonicator at 1000 W for 5 min. Then, ~100 mL of the suspension was passed through the micro-gap of an APV-2000 high-pressure homogenizer (APV, Copenhagen, Denmark), and repeat treated for 20 min.

2.6. TEM observation

TEM images of the cellulose nanofibers and nanofiber bundles were collected using a FEI Tecnai G2 electron microscope at 80 kV acceleration voltages. Drops of dilute cellulose nanofiber suspensions were deposited onto glow-discharged, carbon-coated, electron microscopy grids, then following removal of excess liquid by a piece of filter paper, the sample was air dried at room temperature. Subsequently, a drop of ~2% phosphotungstic acid (PTA) solution was deposited onto the sample for 40–80 s. Later, the excess liquid was removed by a piece of filter paper. The as-prepared sample was air dried at room temperature before TEM observation. Widths of the cellulose nanofibers and nanofiber bundles, which were used to illustrate size distributions, were calculated from the TEM images using a microscope image analysis system (TDY-V5.2, Beijing Tianhong Precision Instrument Technology Co., Ltd., China).

2.7. Scanning electron microscope (SEM)

SEM images were acquired with a scanning electron microscope (Quanta200, FEI, USA).

2.8. Fourier transform infrared (FTIR) spectroscopy

FTIR spectra were recorded on a Fourier transform infrared (FTIR) instrument (Magna 560, Nicolet, Thermo Electron Corp., USA) in the range of 400–4000 cm^{-1} with a resolution of 4 cm^{-1}. The dried samples were ground into powders using a fiber microtome, and then blended with KBr before pressing into ultrathin pellets.

3. Results and discussion

3.1. Preparation of cellulose nanofiber suspensions

The raw wood fibers exhibit rod like structures (Fig. 1a) with yellow color (Fig. 1d). After the removal of lignin and large amounts

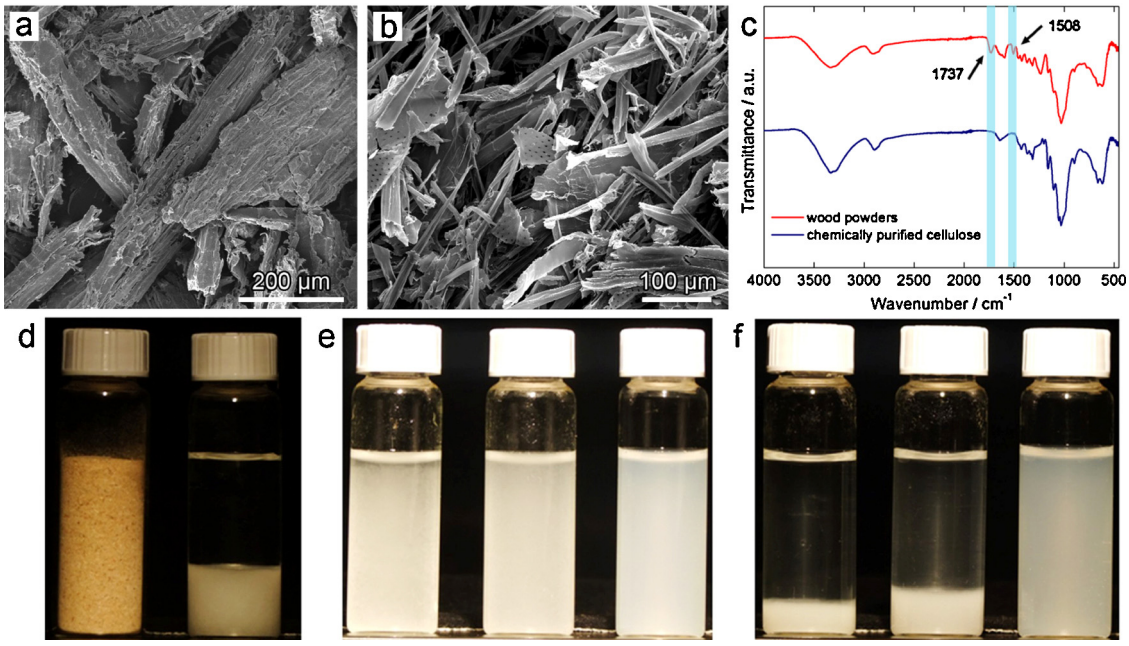

Fig. 1. (a) SEM image of raw wood fibers, (b) SEM image of chemically purified cellulose fibers, (c) FTIR spectra of raw wood fibers and chemically purified cellulose fibers, (d) Photographs of (left) raw wood fibers and (right) chemically purified cellulose fibers, (e and f) Photographs of the cellulose nanofiber suspensions prepared by nanofibrillation the wood cellulose pulps using (left) a blender, (middle) a high intensity ultrasonicator, and (right) a high-pressure homogenizer, respectively. The photographs were taken (e) after just prepared and (f) after set up for more than 10 h.

of hemicelluloses, the samples became white (Fig. 1d). The fibers were split into two different types: fibrous cells and parenchyma cells (Fig. 1b). The FT-IR spectrum of the chemically purified cellulose fibers was quite different from that of the raw wood fibers (Fig. 1c). The peaks at 1508 cm^{-1} (attributed to the C=C stretching vibration in the aromatic ring of lignin) and 1737 cm^{-1} (attributed to either the acetyl and uronic ester groups or the ester linkage of carboxylic group of the ferulic and *p*-coumeric acids of hemicelluloses) were absent in the spectrum of the chemically purified cellulose fibers. This absence indicated that the removal of lignin and large amount of hemicelluloses were achieved by the chemical pre-treatment. The main chemical composition of the resulting sample was cellulose. But, 13–18% hemicellulose was also presented. The hemicellulose has the dual functions of facilitating the disintegration and stabilizing the colloid suspensions. Next, cellulose nanofiber suspensions were prepared by subjecting the chemically purified cellulose fibers to nanofibrillation with a blender, a high intensity ultrasonicator, and a high-pressure homogenizer, respectively. Just after production, all the suspensions were stable and uniform (Fig. 1e); however, the blender- and high intensity ultrasonicator-treated samples were precipitated at the bottom of the bottle after set up for more than 10 h (Fig. 1f). The high pressure homogenizer-treated sample was still stable after set up for 10 h (Fig. 1f) because the nanofibrillation forces introduced by the high-pressure homogenizer were higher than those provided by the blender and high intensity ultrasonicator. The strong nanofibrillation improves the nanofibrillation degree of cellulose pulps, resulting in highly uniform and stable suspensions.

3.2. Structures of cellulose nanofibers

The structures of the cellulose nanofibers were characterized by TEM after negative staining by PTA. The samples obtained via different nanofibrillation methods and from various raw materials exhibit similar morphologies (Fig. 2). TEM images show the presence of very long nanofibers with varying degrees of entanglement. The widths of single nanofibers are mainly in the range of 2–5 nm (Fig. S1). In higher plants, the diameters of single elemental fibrils are reported to be ~3 nm (Somerville et al., 2004). Thus, the slender nanofibers with widths of 2–5 nm are the elemental fibrils isolated from the plant cell walls. The lengths of the single nanofibers exceeded 1 μm, but their ends were difficult to observe because of their entangled, web-like structures.

3.3. Structures of cellulose nanofiber bundles

Large amount of cellulose nanofiber bundles existed in all the suspensions (Figs. 3 and 4). Because the bundles are slender, long and flexible, it is difficult to clearly reveal their structures at any TEM magnifications. However, it is very easy to find a bundle and focus on one end of the bundle during TEM observation. To display the bundle structures vividly, first, high magnification (Magnified higher than 40,000 times) and high resolution TEM images were obtained starting from one end of the bundles. The imaging position was then carefully shifted along the length of the bundles until the other end was reached. Finally, a series of TEM images were integrated through image processing. This resulted in high resolution TEM image of the bundle along its whole length. For the bundles obtained by nanofibrillation the cellulose pulps with a blender, 11 TEM images recorded along the length of a representative bundle were integrated (Fig. 3). The results demonstrate several important points. First, the length of the bundle was around 12.17 μm. Longer bundles were also frequently observed in the suspensions. Second, the bundle was organized of aligned cellulose nanofibers with 2–5 nm widths. The ends of single cellulose nanofibers inside the bundles were also difficult to observe. Third, several individualized nanofibers and slender bundles were attached on the surfaces of the big bundle. Fourth, the bundle was interconnected with other nanofibers and nanofiber bundles, forming a web-like, entangled network in the suspension.

As shown in Fig. 4, the high intensity ultrasonicator-treated and high pressure homogenizer-treated bundles also displayed long and flexible ribbon-like structures. The lengths of high intensity ultrasonicator-treated and high-pressure homogenizer-treated

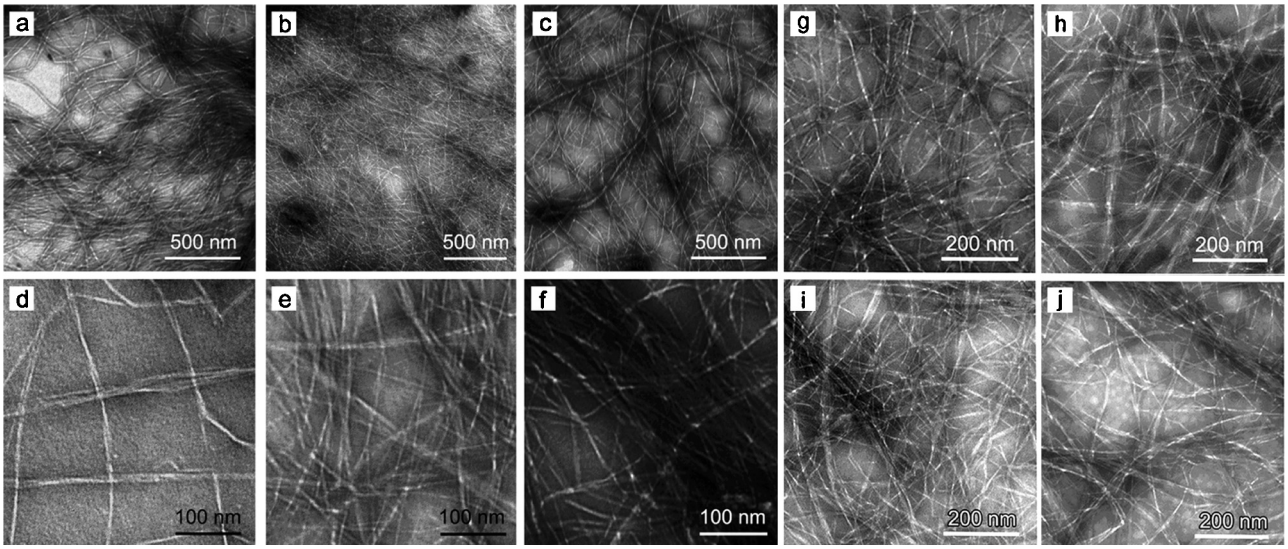

Fig. 2. TEM images of cellulose nanofibers prepared by nanofibrillation the wood cellulose pulps using (a and d) a blender, (b and e) a high intensity ultrasonicator, and (c and f) a high-pressure homogenizer, respectively. TEM images of cellulose nanofibers isolated from (g) bamboo, (h) rice straw, (i) corn stalk and (j) newspaper. The cellulose nanofibers in figures (g)–(j) were prepared by nanofibrillation of the purified cellulose pulps using a high-pressure homogenizer.

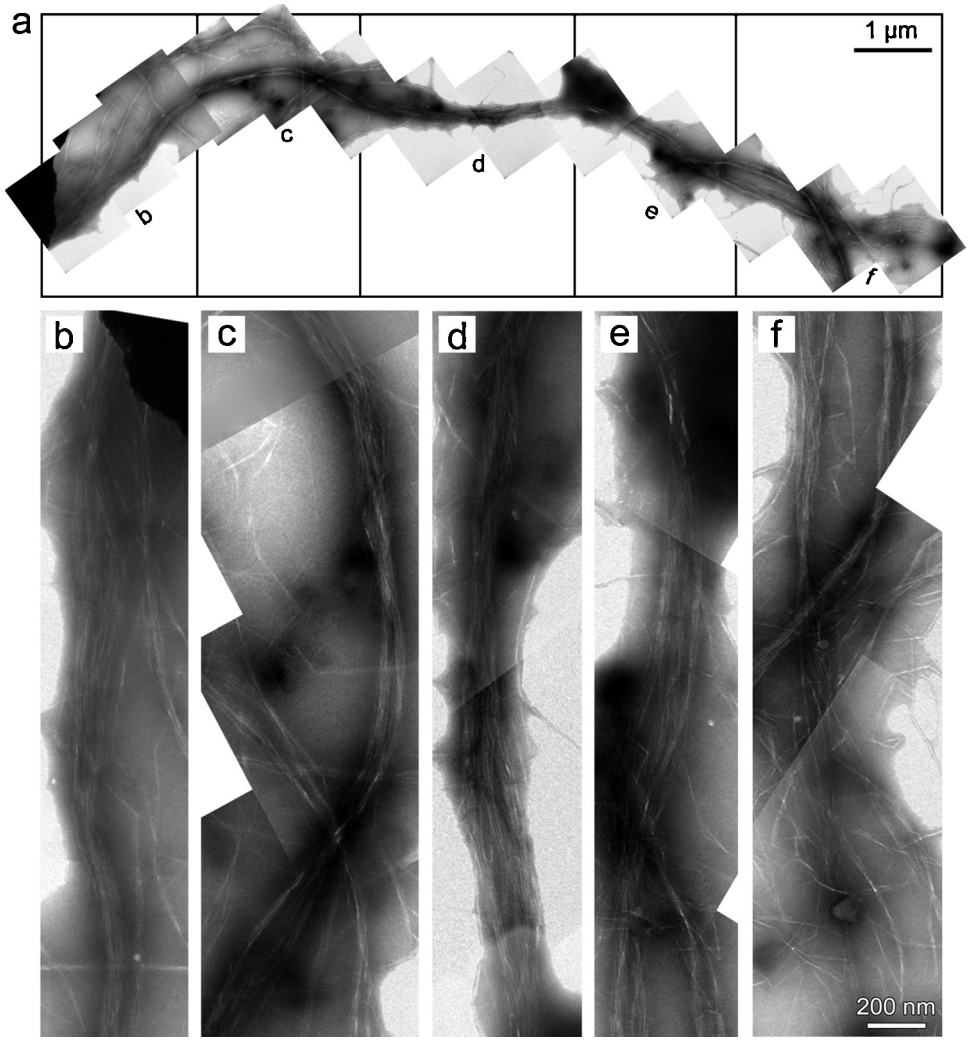

Fig. 3. A series of 13 TEM images of a 12.17 μm-long cellulose nanofiber bundles prepared by nanofibrillation the wood cellulose pulps using a blender. Images of ((b)–(f)) are the high magnification images of (a).

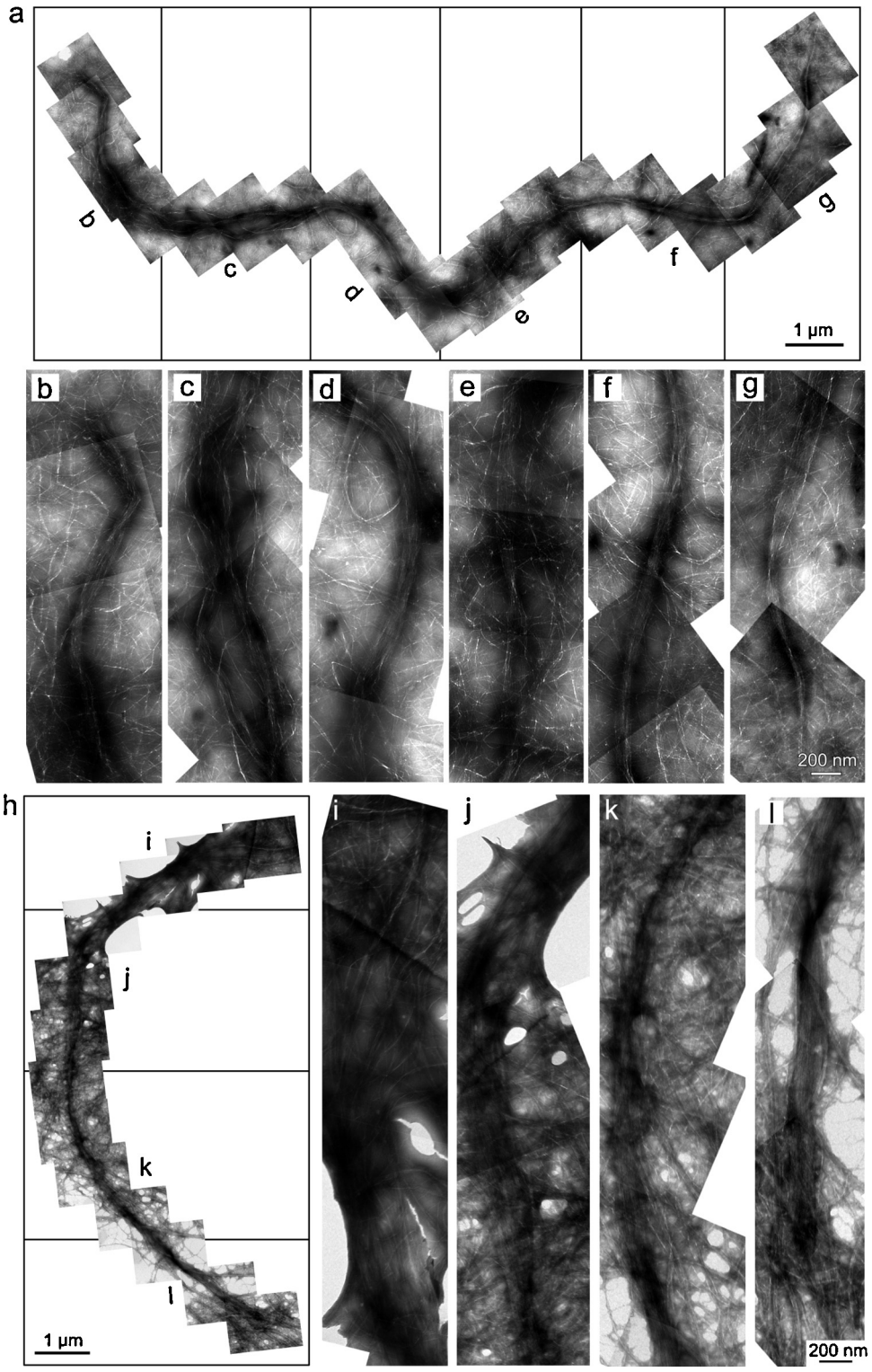

Fig. 4. (a) A series of 20 TEM images of a 18.71 μm-long cellulose nanofiber bundles prepared by nanofibrillation the wood cellulose pulps using a high intensity ultrasonicator. (h) A series of 13 TEM images of a 11.75 μm-long cellulose nanofiber bundles prepared by nanofibrillation the wood cellulose pulps using a high-pressure homogenizer. Images of ((b)–(g)) are the high magnification images of (a). Images of ((i)–(l)) are the high magnification images of (h).

bundles were 18.71 μm and 11.75 μm, respectively. It should be noted that several larger bundles existed in all the samples. Although the different cellulose nanofiber types showed different colloidal behavior and stability (Fig. 1f) because of the differences of the nanofibrillation degree of cellulose pulps, the structures of the 3 kinds of bundles illustrated similar results. The amount of big bundles in the blender-treated and high intensity ultrasonicator-treated samples should be higher than that of high pressure homogenizer-treated samples. But, the bundles were existed in all the samples during or after removal of hemicellulose, or in the colloidal state (because the suspensions were not transparent), or during or after the drying of the colloid suspensions. All the bundles exhibited long ribbon-like structures organized by parallel aligned 2–5 nm width cellulose nanofibers. Bundles were

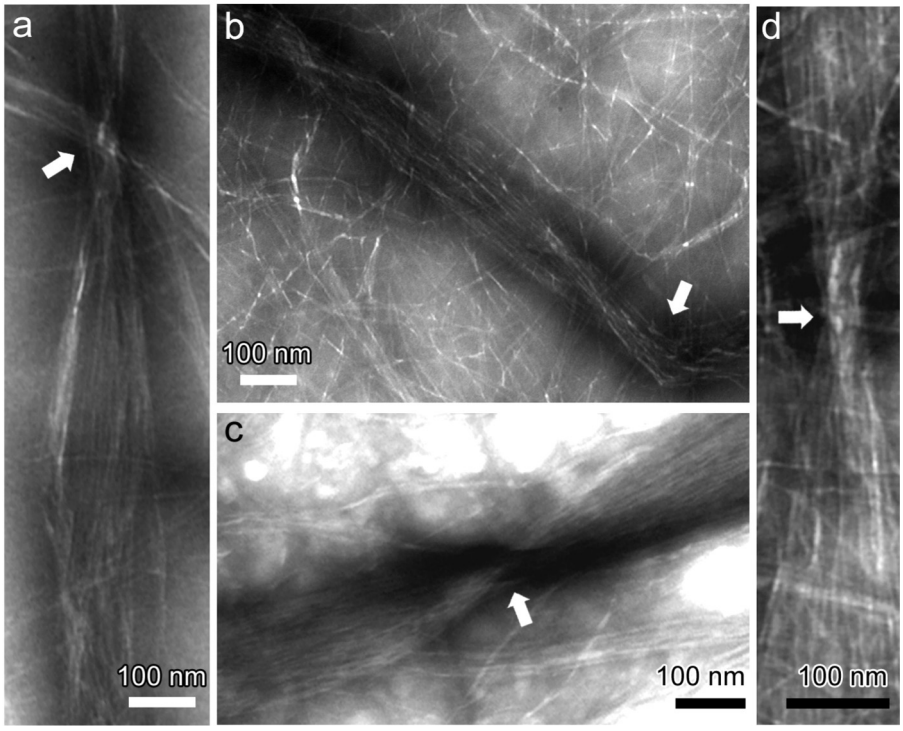

Fig. 5. SEM images of cellulose nanofiber bundles showing twisted morphologies with arrows. The bundles were prepared by nanofibrillation the wood cellulose pulps using (a) a blender, (b) a high intensity ultrasonicator, and (c) a high-pressure homogenizer, respectively. The bundles in (d) were prepared by nanofibrillation the newspaper pulps using a high-pressure homogenizer.

also frequently observed in the suspensions obtained from different raw cellulose resources including bamboo, rice straw, corn straw, newspaper, and many others.

3.4. Twisted morphologies of cellulose naofiber bundles

Observations of the cellulose nanofiber bundles along their lengths show that the bundles exhibit twisted morphologies (Fig. 5). The twisting tendency is identified in images of bundles obtained from differently nanofibrillation methods and raw materials. In the TEM images, twisted regions are visible at intervals. There are several torsion points along the lengths of the bundles. The 'top' surface of the ribbon-like bundle twists ~180° and transforms to the 'bottom' surface when it crosses the torsion point. The apparent differences between the two sides of the torsion points clearly illustrate the twisting tendency of the cellulose nanofiber bundles. The bundles thus appear to be flat ribbons with twist morphologies organized by parallel aligned cellulose nanofibers.

The fact that microfibrils within the cell walls of cellulosic materials tend to twist has long been recognized. For instance, the twisting process has been observed during the biosynthesis of bacterial cellulose (Brown et al., 1983). Khandelwal and Windle (2014) also provided evidence to support the twisted structure of bacterial cellulose microfibrils. Grey et al. reported that individual microfibrils of green alga (*Micrasterias denticulate*) show a strong tendency to twist in a right-handed manner (Hanley et al., 1997). The microfibrils in the plant cell walls (especially at the S_2 layer) twist and rotate to form the higher-order structures of cell walls. Therefore, the twist structures of cellulose nanofiber bundles are originated from their natural twisted structures within the plant cell walls.

4. Conclusion

In summary, the structures of cellulose nanofiber bundles were systematically investigated by the integration of a series of TEM images recorded along the length of the bundles. The bundles were formed during or after removal of hemicellulose, or in the colloidal state, or during or after the drying of the colloid suspensions. Although the different cellulose nanofiber types showed different colloidal behavior and stability, the bundles obtained from different nanofibrillation methods and raw materials exhibited similar ribbon-like structures organized by parallel aligned cellulose nanofibers with 2–5 nm widths. The length of the bundles was >11 μm. Single nanofibers or slender bundles were also attached on the surfaces of the bundles. The bundles and individualized cellulose nanofibers were cross-linked with each other and formed entangled, web-like structures. The twisted structures of the bundles were also revealed from the TEM images.

Acknowledgements

This work was supported in part by the Fundamental Research Funds for the Central Universities (DL13BBX05), the Postdoctoral Science-Research Developmental Foundation of Heilongjiang Province of China (LBH-Q12162), and the National Natural Science Foundation of China (31270590).

Appendix A. Supplementary data

Supplementary data associated with this article can be found, in the online version, at http://dx.doi.org/10.1016/j.carbpol.2014.10.024.

References

Abe, K., Iwamoto, S., & Yano, H. (2007). Obtaining cellulose nanofibers with a uniform width of 15 nm from wood. *Biomacromolecules*, *8*(10), 3276–3278.
Abe, K., & Yano, H. (2009). Comparison of the characteristics of cellulose microfibril aggregates of wood, rice straw and potato tuber. *Cellulose*, *16*(6), 1017–1023.
Abe, K., & Yano, H. (2010). Comparison of the characteristics of cellulose microfibril aggregates isolated from fiber and parenchyma cells of Moso bamboo (*Phyllostachys pubescens*). *Cellulose*, *17*(2), 271–277.

Brown, R. M., Jr., Haigler, C. H., Suttie, J., White, A. R., Roberts, E., Smith, C., et al. (1983). The biosynthesis and degradation of cellulose. *Journal of Applied Polymer Science: Applied Polymer Symposium*, *37*, 33–78.

Capadona, J. R., Shanmuganathan, K., Tyler, D. J., Rowan, S. J., & Weder, C. (2008). Stimuli-responsive polymer nanocomposites inspired by the sea cucumber dermis. *Science*, *319*(5868), 1370–1374.

Capadona, J. R., Van Den Berg, O., Capadona, L. A., Schroeter, M., Rowan, S. J., Tyler, D. J., et al. (2007). A versatile approach for the processing of polymer nanocomposites with self-assembled nanofibre templates. *Nature Nanotechnology*, *2*(12), 765–769.

Chen, W., Li, Q., Wang, Y., Yi, X., Zeng, J., Yu, H., et al. (2014). Comparative study of aerogels obtained from differently prepared nanocellulose fibers. *ChemSusChem*, *7*(1), 154–161.

Chen, W., Yu, H., Li, Q., Liu, Y., & Li, J. (2011). Ultralight and highly flexible aerogels with long cellulose I nanofibers. *Soft Matter*, *7*(21), 10360–10368.

Chen, W., Yu, H., Liu, Y., Chen, P., Zhang, M., & Hai, Y. (2011). Individualization of cellulose nanofibers from wood using high-intensity ultrasonication combined with chemical pretreatments. *Carbohydrate Polymers*, *83*(4), 1804–1811.

Chen, W., Yu, H., Liu, Y., Hai, Y., Zhang, M., & Chen, P. (2011). Isolation and characterization of cellulose nanofibers from four plant cellulose fibers using a chemical-ultrasonic process. *Cellulose*, *18*(2), 433–442.

Eichhorn, S. J. (2011). Cellulose nanowhiskers: Promising materials for advanced applications. *Soft Matter*, *7*(2), 303–315.

Habibi, Y., Lucia, L. A., & Rojas, O. J. (2010). Cellulose nanocrystals: Chemistry, self-assembly, and applications. *Chemical Reviews*, *110*(6), 3479–3500.

Hanley, S. J., Revol, J.-F., Godbout, L., & Gray, D. G. (1997). Atomic force microscopy and transmission electron microscopy of cellulose from Micrasterias denticulata; evidence for a chiral helical microfibril twist. *Cellulose*, *4*(3), 209–220.

Herrick, F. W., Casebier, R. L., Hamilton, J. K., & Sandberg, K. R. (1983). Microfibrillated cellulose: Morphology and accessibility. *Journal of Applied Polymer Science: Applied Polymer Symposium*, *37*, 797–813.

Isogai, A. (2013). Wood nanocelluloses: Fundamentals and applications as new bio-based nanomaterials. *Journal of Wood Science*, *59*(6), 449–459.

Isogai, A., Saito, T., & Fukuzumi, H. (2011). TEMPO-oxidized cellulose nanofibers. *Nanoscale*, *3*(1), 71–85.

Kelly, J. A., Giese, M., Shopsowitz, K. E., Hamad, W. Y., & MacLachlan, M. J. (2014). The Development of chiral nematic mesoporous materials. *Accounts of Chemical Research*, *47*(4), 1088–1096.

Khandelwal, M., & Windle, A. (2014). Origin of chiral interactions in cellulose supramolecular microfibrils. *Carbohydrate Polymers*, *106*, 128–131.

Klemm, D., Kramer, F., Moritz, S., Lindström, T., Ankerfors, M., Gray, D., et al. (2011). Nanocelluloses: A new family of nature-based materials. *Angewandte Chemie International Edition*, *50*(24), 5438–5466.

Metreveli, G., Wågberg, L., Emmoth, E., Belák, S., Strømme, M., & Mihranyan, A. (2014). A size-exclusion nanocellulose filter paper for virus removal. *Advanced Healthcare Materials*, http://dx.doi.org/10.1002/adhm.201300641

Moon, R. J., Martini, A., Nairn, J., Simonsen, J., & Youngblood, J. (2011). Cellulose nanomaterials review: Structure, properties and nanocomposites. *Chemical Society Reviews*, *40*(7), 3941–3994.

Nogi, M., Iwamoto, S., Nakagaito, A. N., & Yano, H. (2009). Optically transparent nanofiber paper. *Advanced Materials*, *21*(16), 1595–1598.

Nogi, M., & Yano, H. (2008). Transparent nanocomposites based on cellulose produced by bacteria offer potential innovation in the electronics device industry. *Advanced Materials*, *20*(10), 1849–1852.

Olsson, R. T., Samir, M. A., Salazar-Alvarez, G., Belova, L., Ström, V., Berglund, L. A., et al. (2010). Making flexible magnetic aerogels and stiff magnetic nanopaper using cellulose nanofibrils as templates. *Nature Nanotechnology*, *5*(8), 584–588.

Pääkkö, M., Ankerfors, M., Kosonen, H., Nykänen, A., Ahola, S., Österberg, M., et al. (2007). Enzymatic hydrolysis combined with mechanical shearing and high-pressure homogenization for nanoscale cellulose fibrils and strong gels. *Biomacromolecules*, *8*(6), 1934–1941.

Pääkkö, M., Vapaavuori, J., Silvennoinen, R., Kosonen, H., Ankerfors, M., Lindström, T., et al. (2008). Long and entangled native cellulose I nanofibers allow flexible aerogels and hierarchically porous templates for functionalities. *Soft Matter*, *4*(12), 2492–2499.

Shopsowitz, K. E., Qi, H., Hamad, W. Y., & MacLachlan, M. J. (2010). Free-standing mesoporous silica films with tunable chiral nematic structures. *Nature*, *468*(7322), 422–425.

Siró, I., & Plackett, D. (2010). Microfibrillated cellulose and new nanocomposite materials: A review. *Cellulose*, *17*(3), 459–494.

Somerville, C., Bauer, S., Brininstool, G., Facette, M., Hamann, T., Milne, J., et al. (2004). Toward a systems approach to understanding plant cell walls. *Science*, *306*(5705), 2206–2211.

Turbak, A. F., Snyder, F. W., & Sandberg, K. R. (1983). Microfibrillated cellulose, a new cellulose product: Properties, uses, and commercial potential. *Journal of Applied Polymer Science: Applied Polymer Symposium*, *37*, 815–827.

Uetani, K., & Yano, H. (2010). Nanofibrillation of wood pulp using a high-speed blender. *Biomacromolecules*, *12*(2), 348–353.

Uetani, K., & Yano, H. (2013). Self-organizing capacity of nanocelluloses via droplet evaporation. *Soft Matter*, *9*(12), 3396–3401.

Yano, H., Sugiyama, J., Nakagaito, A. N., Nogi, M., Matsuura, T., Hikita, M., et al. (2005). Optically transparent composites reinforced with networks of bacterial nanofibers. *Advanced Materials*, *17*(2), 153–155.

Zhao, H. P., Feng, X. Q., & Gao, H. (2007). Ultrasonic technique for extracting nanofibers from nature materials. *Applied Physics Letters*, *90*(7), 073112.